ACS NANO

www.acsnano.org

PERSPECTIVE

One-Dimensional Atomic Chains for Ultimate-Scaled Electronics

You Meng, Wei Wang, and Johnny C. Ho*

Cite This: *ACS Nano* 2022, 16, 13314–13322

Read Online

ACCESS | Metrics & More | Article Recommendations

ABSTRACT: **The continuous downscaling of semiconducting channels in transistors has driven the development of modern electronics. However, with the component transistors becoming smaller and denser on a single chip, the continued downscaling progress has touched the physical limits. In this Perspective, we suggest that the emerging one-dimensional (1D) material system involving inorganic atomic chains (ACs) that are packed by van der Waals (vdW) interactions may tackle this issue. Stemming from their 1D crystal structures and naturally terminated surfaces, 1D ACs could potentially shrink transistors to atomic-scale diameters. Also, we argue that 1D ACs with few-atom widths allow us to revisit 1D materials and uncover physical properties distinct from conventional materials. These ultrathin 1D AC materials demand substantive attention. They may bring opportunities to develop ultimate-scaled AC-based electronic, optoelectronic, thermoelectric, spintronic, memory devices, etc.**

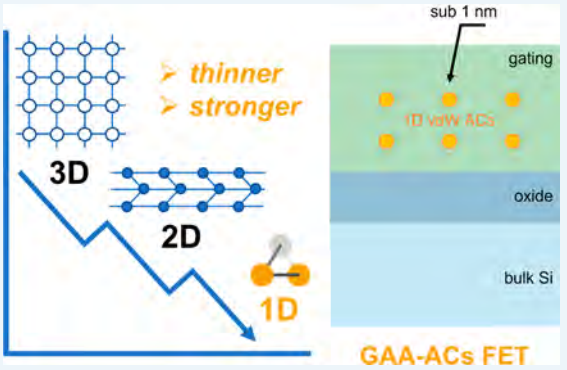

KEYWORDS: *one-dimensional, atomic chain, electronic, van der Waals interaction, downscaling*

INTRODUCTION

Powered by the relentless device miniaturization, field-effect transistors (FETs) have served as the primary building blocks for nowadays information technology.[1,2] In order to obtain a smaller device size, better gate coupling, and lower power consumption, silicon (Si) FET technology has been rapidly developed in the past decades following Moore's Law, with the transistor density on a single chip doubling about every two years.[3,4] At the same time, the miniaturization of FETs witnessed the structural evolutions from planar to fin-shaped and all the way to gate-all-around (GAA) device geometries (Figure 1a), with the corresponding feature sizes downscaling from tens of nanometers to a few nanometers. Due to the limitation of nanofabrication precision and short-channel effects, it is now highly challenging to further shrink the size of transistors approaching molecular or atomic levels (Figure 1b).[5−7] On the other hand, with the continuous downscaling of transistor size, the Si bandgap dramatically increases, and the surface scattering becomes dominant,[8] being detrimental to the charge carrier transport. Consequently, to satisfy the device miniaturization requirements of nanometer or even sub-nanometer electronics, all of the critical factors governing the downscaling device process must be carefully considered, such as materials, architectures, and concepts.

The emerging nanomaterials with definite geometrical and electronic structures can potentially fulfill the technological demands on device miniaturization, multifunctionality, and precise fabrication.[9] The advent of van der Waals (vdW) materials, such as the well-known two-dimensional (2D) layered materials, has led to progress in their fundamental research and practical applications.[10,11] Taking one more step down in dimensionality, from 2D monolayers to one-dimensional (1D) atomic chains (ACs), it would touch the ultimate limit in material downscaling and establish a research field of 1D AC materials and associated applications. Analogous to 2D layered materials, the inorganic 1D ACs are also packed by vdW interactions and free of surface dangling bonds (Figure 1c). At the same time, in each AC, the covalent-bonded atoms are sequenced along the chain direction. Also, inorganic 1D ACs with few-atom diameters, corresponding to the smallest 1D structures with intrinsically structural anisotropy and super material performance, may

Received: June 28, 2022
Accepted: August 16, 2022
Published: August 23, 2022

https://doi.org/10.1021/acsnano.2c06359
ACS Nano 2022, 16, 13314–13322

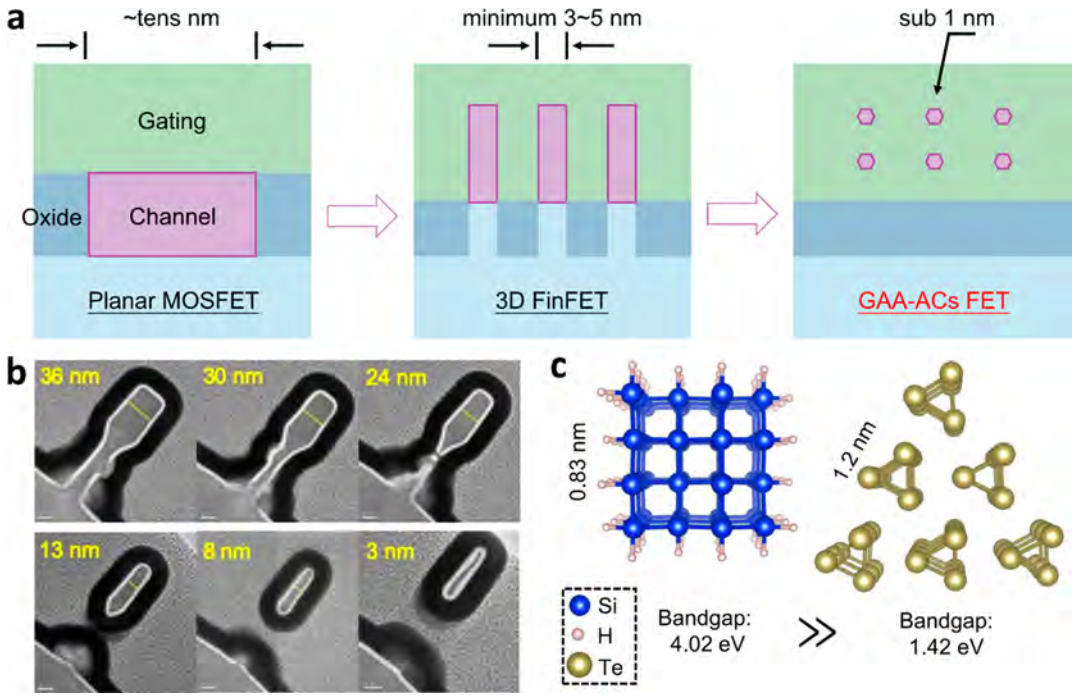

Figure 1. Structural evolutions of FET devices and their semiconducting channels. (a) Schematic illustration of device structure evolutions from planar MOSFET to 3D FinFET to future GAA-AC FETs. (b) Cross-section TEM images of GAA InGaAs channels with different widths from 36 to 3 nm. Image b was reproduced with permission from ref 7. Copyright 2019 ACS. (c) Structural and bandgap comparisons between Si NWs (0.83 nm width) and Te ACs (1.2 nm width). Image c was reprinted with permission under a Creative Commons CC BY License from ref 8. Copyright 2020 Springer Nature.

attract broad research interest in materials, physics, and electronics.

STRUCTURAL ANALYSIS

The 1D ACs have diameters close to carbon nanotubes (CNTs) but with diverse elemental components and crystal structures, by which various material properties ranging from insulator to semiconductor to conductor can be designed and obtained. This versatile flexibility endows 1D AC blocks with precise geometrical and electronic structures, which are highly desirable for assembling functional electronics. Although CNTs have ultrathin 1D morphology and good electrical properties, they have been limited by the random chirality and coexisting metallic/semiconductor characteristics.[12] Besides, traditional crystalline semiconductor (e.g., group III−V and II−VI) nanowires (NWs), with the smallest diameters of a few nanometers, would degrade in material properties induced by surface dangling bonds.[13−15] In contrast, the 1D ACs packed by vdW interactions are promising for next-generation ultimate-scaled devices due to their few-atom widths and naturally terminated surfaces. Some inorganic 1D AC systems have been experimentally synthesized, including elemental chains, transition metal chalcogenides, and transition metal halides. Impressively, hundreds of predicted cases are uncovered by data mining of crystal structure databases and waiting to be experimentally obtained.[16−18]

Without any chemical complexity introduced by the multicompositions, elemental materials are pure and intrinsically homogeneous, promising for denser device integration. It is promising that elemental ACs composed of tellurium (Te),[19−21] selenium (Se),[22] sulfur (S),[23] phosphorus,[24] and carbon[25,26] were experimentally reported. As a kind of "DNA-like" spiral ACs from group 16, hexagonal-packed Te and Se ACs demonstrated good environmental stability and high hole mobility,[19] whereas the 1D S ACs showed conducting behavior.[23] Especially, from first-principles simulations, ultrathin Te ACs with a 1.2 nm diameter have an energy bandgap of ∼1.42 eV (Figure 1c),[8] much lower than Si (∼4.02 eV) with the same size, making Te ACs an ideal semiconducting channel for high-mobility extremely scaled transistors. Carbon exists in many different allotropes, including 3D diamond, 2D graphite, and 1D carbyne, featuring sp^3-, sp^2-, and sp-hybrid orbitals, respectively. Among them, carbyne is the one composed of only 1D carbon ACs, where vdW interactions occur between these kinked carbyne chains, endowing it with potential as a 1D vdW carbon material.[25,26] Theoretically, 1D carbyne ACs have higher strength (7.5×10^7 N·m/kg), elastic modulus (32.7 TPa), and stiffness (95.56 eV/Å) than those of diamond or graphene, allowing them to function as enhanced composite materials or be used in ultraflexible electronics.[27] More importantly, the unexplored carbyne AC electronics with the recorded narrow channel of one-carbon-atom size is waiting to be achieved.[28]

Transition metal chalcogenides (TMCs) made for 1D ACs have been configured with different stoichiometries and structures. Also, the TMC family is a rich material library for ACs, including M_6X_6 (e.g., W_6Te_6 and Mo_6Se_6),[29,30] M_2X_3 (e.g., Bi_2S_3 and Sb_2Se_3),[31,32] MX_3 (e.g., TiS_3 and $NbTe_3$),[33,34] Nb_2Se_9,[35] and $M_2X_3Y_8$ (M = Ta, Nb; X = Ni, Pd, Pt; Y = S, Se) ACs.[36,37] Taking the TMC ACs in the form of M_6X_6 (X = S, Se, Te) as an example, they have 66 1D systems that have the stable 1D crystal structure.[38] These 1D M_6X_6 ACs, consisting of the backbone chain of transition-metal atoms covered by chalcogen atoms, generally exhibit metallic behaviors (except for three semiconducting Cr_6Te_6, Mo_6Te_6, and W_6Te_6), which is mainly because of the strong hybridization between

https://doi.org/10.1021/acsnano.2c06359
ACS Nano 2022, 16, 13314−13322

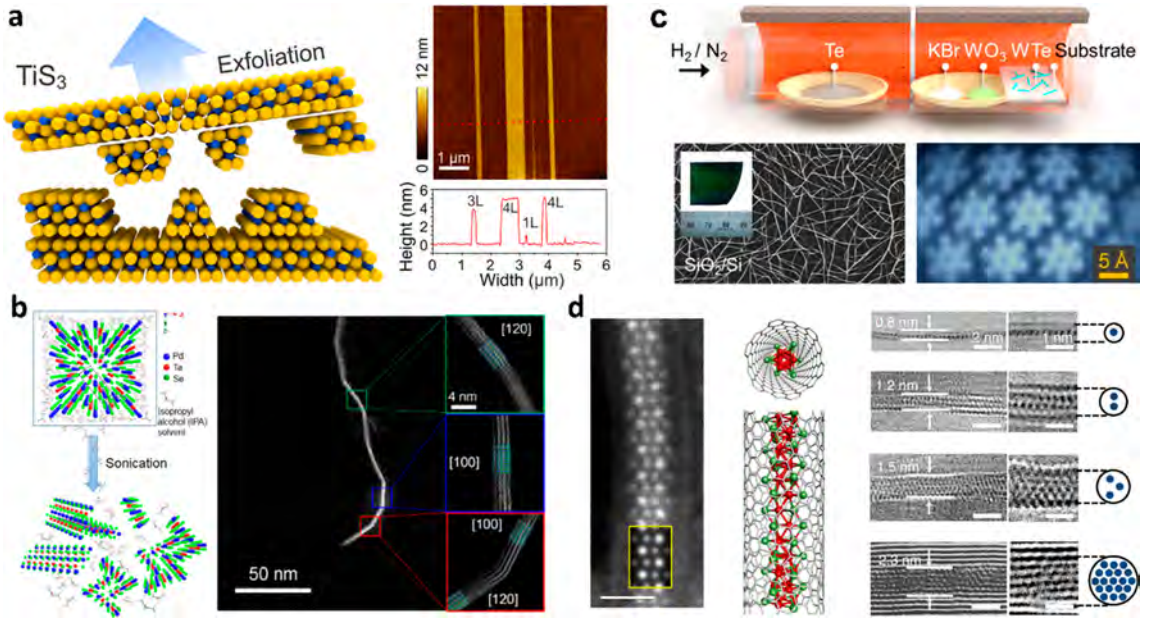

Figure 2. Formation pathway and crystal structures of 1D AC materials. (a) Mechanical exfoliation of TiS_3 ACs and the corresponding AFM image and height profile after exfoliation. Image a was reproduced with permission from ref 33. Copyright 2018 ACS. (b) Liquid-phase exfoliation of $Ta_2Pd_3Se_8$ ACs and the corresponding STEM image after exfoliation. Image b was reproduced with permission from ref 50. Copyright 2020 Springer Nature. (c) CVD-grown W_6Te_6 or Mo_6Te_6 ACs and the corresponding optical, SEM, and cross-sectional STEM images. Image c (top and bottom left) was reproduced with permission from ref 51. Copyright 2020 ACS. Image c (bottom right) was reproduced with permission from ref 52. Copyright 2020 ACS. (d) (left) STEM image and (middle) atomic structural model of Mo_6Te_6 ACs encapsulated inside CNTs. Image d (left and middle) was reproduced with permission from ref 56. Copyright 2019 ACS. (right) HRTEM images of Te ACs encapsulated inside CNTs with different chain numbers. Image d (right) was reproduced with permission from ref 19. Copyright 2020 Springer Nature.

transition-metal d orbitals and chalcogen p orbitals. In contrast, the 2D layered TMC systems in the 2H phase are commonly semiconductors. In this case, exploring the phase transition, mechanical deformation, alloying, and doping effects on the physical properties of TMC ACs, especially the possibility of bandgap opening, is essential. To date, most successful experimental studies focused only on the limited TMC ACs with component elements analogous to their 2D layered counterparts, i.e., Mo-based chalcogenides and W-based chalcogenides. The question is whether the other transition metal elements besides Mo and W can form useful 1D ACs. What would be their geometrical structures and electronic configurations if this is the case? Certainly, more kinds of TMC 1D ACs with tunable physical properties are coming, which is expected to cover a broader scope than their monolayer 2D counterparts.

Besides, transition metal halides (TMHs) generally involve nontoxic and earth-abundant elements, suitable for low-cost and low-temperature synthesis. There exist some TMHs with intrinsic 1D crystal structures in stoichiometries of MX_2 (e.g., $CrCl_2$, $NiBr_2$, and CoI_2)[39,40] and MX_3 (e.g., $TiCl_3$, $RuBr_3$, and $MoBr_3$),[41,42] wherein each chain of transition metal atoms is bridged by four and six halogen atoms, respectively. From the calculated energetic view, TMH 1D ACs in the form of MX_3 are generally more stable than MX_2 ACs, while the F-based TMHs are more stable than the other TMH ACs.[43] As for material properties, there is less understanding of TMH ACs compared to TMC ACs. However, based on the existing findings of TMH ACs, this 1D material family is still attractive for applications, owing to their diverse electronic properties, where they can be configured in semiconductors, ferromagnets, antiferromagnets, and semimetals. In contrast to TMC ACs that usually exhibit metallic behaviors, most TMH ACs are semiconductors (e.g., 58 MX_2 and 86 MX_3) with bandgaps widely manipulated from 0.10 to 6.71 eV,[43] thereby promising for electronic, optoelectronic, and light-harvesting devices. For most of the 1D TMH semiconductors, their effective masses of electron carriers are calculated to be below 0.3 m_0,[43] suggesting that the electron carriers are highly mobile, being useful for fast electronics. Among them, some TMH ACs, such as MBr_3 (M = Sc, Y), IrX_3, and RhX_3 ACs with bandgaps of 1.55−2.99 eV, show a strong light absorption intensity up to 10^5 cm^{-1}, covering the ultraviolet and visible regime, highlighting their capability to capture solar energy.[43] Nevertheless, the comprehensive understanding between electronic configurations and compositions in TMH 1D ACs has not been fully achieved and thus requires detailed investigation, especially for practical device utilizations like transistors.

FORMATION PATHWAY

The downscaling evolution of low-dimensional semiconducting materials, morphing from 3D to 2D to 1D, witnessed the development of nanotechnology.[9] The nanoscale materials often reveal properties not seen in their bulk crystals, mainly resulting from the confinement and surface effects.[29,44,45] The development of feasible and reliable methods for preparing 1D AC materials is important to study their material properties and device applications. The vdW interactions among 1D ACs would potentially facilitate the synthesis, isolation, and assembly of ACs, though the challenges remained. As shown in Figure 2, extensive efforts have been devoted to exploring different kinds of 1D AC synthetic strategies, including top-down, bottom-up, and nanotemplate approaches.

https://doi.org/10.1021/acsnano.2c06359
ACS Nano 2022, 16, 13314−13322

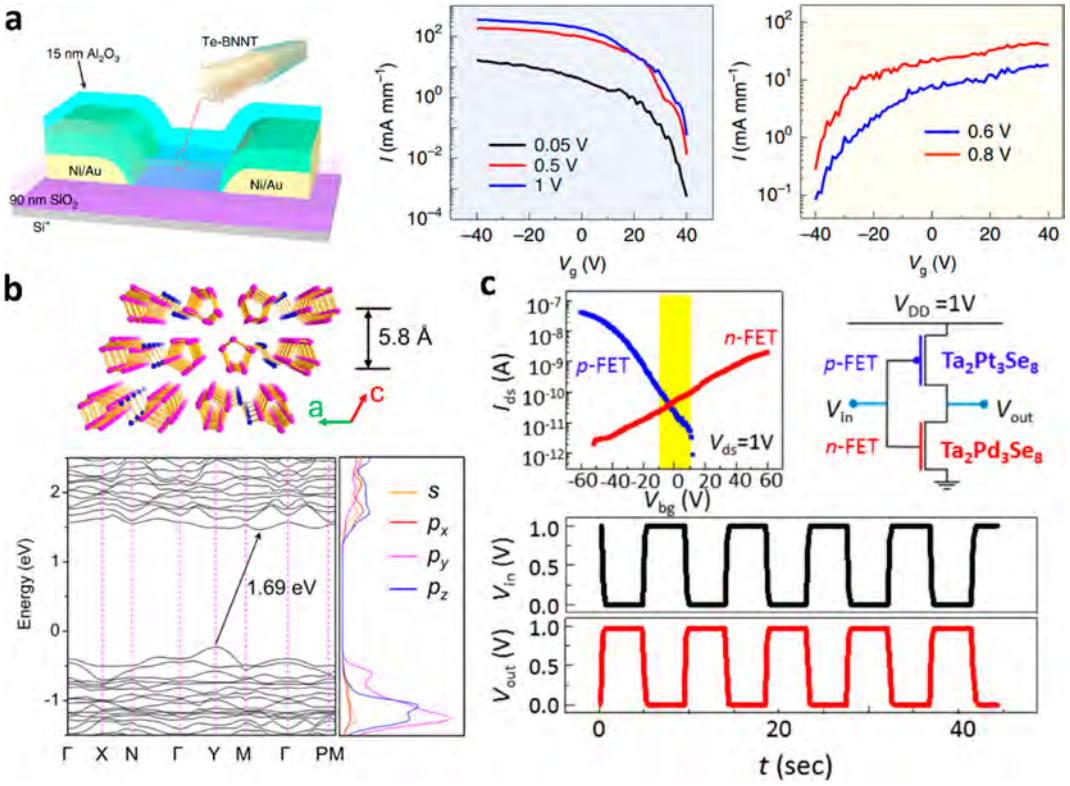

Figure 3. Electronics based on various 1D ACs. (a) (left) Device structure and transfer characteristics of few-chain Te AC transistors (middle) before and (right) after Al_2O_3 film capping. Image a was reproduced with permission from ref 19. Copyright 2020 Springer Nature. (b) (top) Crystal structure and (bottom) calculated electronic structure of fibrous RP. Image b was reproduced with permission from ref 24. Copyright 2021 ACS. (c) The logic NOT gate built with p-type $Ta_2Pt_3Se_8$ FET and n-type $Ta_2Pd_3Se_8$ FET. Image c was reproduced with permission from ref 72. Copyright 2016 ACS.

The top-down approach relies on isolating bulk crystals into few-chain or even single-chain ACs, in which different driving forces are utilized to break the weak vdW interactions among the stacked chains. The simulation results indicate that the out-of-plane cleavage energy of 1D vdW crystals is close to or even lower than that of layered graphene.[46] Taking 1D MX_3 (M = Ti, Zr; X = S, Se, Te) as an example, the cleavage energy between chains is 0.2−0.7 J m^{-2}, which is much lower than that along the chains of 2.9−3.1 J m^{-2}.[33,47] In this regard, it is practical to identify the appropriate experimental parameters for the mechanical or chemical exfoliations of individual ACs from their bulk counterparts. Following this idea, mechanical or liquid-phase exfoliations of Te,[48] TiS_3 (Figure 2a),[33] Nb_2Se_9,[35] $Ta_2Ni_3Se_8$,[36] $Ta_2Pt_3Se_8$,[49] and $Ta_2Pd_3Se_8$ (Figure 2b)[50] few-chain ACs were realized with diameters down to ∼1 nm. These exfoliated 1D ACs exhibit good electrical switching performance and thickness-dependent properties, e.g., bandgap opening and indirect-to-direct bandgap transition. Unlike the liquid-phase or ion-intercalation exfoliation, there are no chemical reactions or organic ligand additions that occurred during the mechanical exfoliation process. The mechanically exfoliated 1D AC materials would remain in the same crystal structures as their bulk counterparts and keep good quality with few defects. Thus, the mechanical exfoliation is ideal for easy accessibility to 1D ACs with different thicknesses, being facile and convenient to screen suitable active channels for functional utilization and study their intrinsic properties. Nonetheless, the mechanical exfoliation in its current form still has limitations in the production yield and morphology control (e.g., thickness, size, and shape), restricting their large-area practical applications.

Compared to the top-down approach, the on-demand bottom-up method allows better control of AC growth with preserved structural integrity and good homogeneity. The bottom-up process directly synthesizes ultrathin 1D ACs on target substrates under certain experimental conditions. For instance, the wafer-scale fabrication of highly crystalline ultrathin W_6Te_6 (or Mo_6Te_6) NWs, composed of individual ACs, has been demonstrated by chemical vapor deposition (CVD) on SiO_2 substrates (Figure 2c).[51,52] Ultrahigh vacuum molecular beam epitaxy (UV-MBE) was also employed to fabricate the isolated single W_6Te_6 ACs on the bilayer graphene (BLG) substrate, featuring an opening bandgap of ∼60 meV.[29] In addition, conducting M_6X_6 (M = Mo or W; X = S or Se) and its alloying ACs, with a thickness down to 1 nm, were also produced by selected-area ionization reaction of semiconducting MX_2 monolayer counterparts using a focused low-energy electron beam (60 kV).[30,53] Bottom-up methods are demonstrated to be generic and effective for fabricating numerous nanomaterials, where high growth temperature and high vacuum are commonly needed for good material qualities.[14,54,55] Bearing this in mind, the low-temperature bottom-up growth of ultrathin 1D ACs on arbitrary substrates is the key to solving the cost-effectiveness issue of devices.

In any case, isolating 1D ACs with atomic preciseness is more complicated than manipulating 2D monolayers. Moreover, atomically thin samples are highly air-sensitive and easy to decompose. In order to tackle the stability problems, few-chain or even single-chain ACs were directly encapsulated into

https://doi.org/10.1021/acsnano.2c06359
ACS Nano 2022, 16, 13314−13322

CNTs, boron nitride nanotubes (BNNTs), or zeolite pores,[22] and the related techniques have been applied to various 1D ACs, including carbyne,[25] Te,[19] Se,[22] CoI_2,[39] $TiTe_3$,[34] and Mo_6Te_6.[56] Using this method, the AC numbers can be tuned by the inner diameter of the nanotemplate (Figure 2d). In particular, the nanoscale spatial confinement stabilizes the $NbSe_3$ AC growth to triple, double, and even single chains, subsequently contributing to the 1D electron and phonon transport.[57] Besides, the single SnSe ACs encapsulated inside single-walled CNTs generate different crystalline forms as designed, including linear, zigzag, and helical (2 × 1) ACs.[58] The nanotemplate approaches also allow us to explore the fundamental physics and chemistry based on 1D ACs, such as strain-mediated chain distortion,[59] supermodulation of ordered defects,[60] and selective phase transition.[61] On the other hand, nanotemplate encapsulation blocks the 1D ACs from environmental-factor-induced degradations, enabled by the chemically inert nature of the nanotemplate shell. However, the passivation shell layer also possibly restricts using these buried ACs directly. To bypass this issue, employing growth nanotube shells as functional layers is feasible, e.g., using BN nanotube shells as dielectric layers of GAA-AC transistors.

ELECTRONICS OF ATOMIC CHAINS

Because of the good immunity to short-channel effects and dangling-bond-free surfaces, 1D AC materials would provide opportunities for achieving the ultimate-scaled transistors. Besides, the ultrathin 1D ACs are highly sensitive to external stimuli, such as strain, light, thermal, magnetic, electric, and electrostatic effects, allowing us to regulate their electronic properties in the desired manner. As a result, the 1D ACs would support promising utilization in not only electronic but also photonic, optoelectronic, thermoelectric, spintronic, and memory devices.

Most inorganic semiconductors are n-type, while most organic semiconductors are p-type. As complementary electronics require both types of semiconductors, the researchers have intensively strived to fill the technology gap of exploring high-performance inorganic p-type semiconductors. Interestingly, many inorganic 1D ACs are p-type semiconductors with good hole mobility. For example, a p-type GAA-NW FET was demonstrated using a Te NW as the semiconducting channel and BN as the insulating dielectric.[62] With reasonable electrostatic control, a field-effect hole mobility of 1390 $cm^2\ V^{-1}\ s^{-1}$ was obtained, which surpasses the state-of-the-art hole mobility of strained Si. Few-chain Te ACs could also be isolated in BN nanotubes for electronic applications with a diameter of only 2 nm,[19] by which a current-carrying capacity of 1.5×10^8 A cm^{-2} was obtained that exceeds most semiconducting NWs. In the same work, it was shown that the atomic-layer-deposited Al_2O_3 capping layer can modulate the transistor behaviors from p-type to n-type (Figure 3a), enabled by the surface charge transfer doping process. These findings have intriguing prospects for next-generation electronics with alternate channel materials. It is also noted that the theoretical hole mobilities of Te materials are up to $\sim 10^5\ cm^2\ V^{-1}\ s^{-1}$,[63] owing to the low effective mass and narrow bandgap. Thus, it is promising to further improve the mobility of 1D Te AC materials in the future with various strategies, such as surface doping,[19,44] composition design,[64] and dielectric engineering.[65]

At the same time, elemental phosphorus is abundant, readily available, and environmentally friendly. Among many of their allotropes, including white phosphorus, red phosphorus (RP), and black phosphorus, RP is the major form and kinetically most stable one.[66,67] More importantly, the RP crystal is a 1D chain-like material packed by vdW interactions (Figure 3b). Semiconducting RP materials have been successfully fabricated using chemical vapor transport,[24] thermal evaporation,[68] or spin coating.[69] It is impressive that the FET devices based on exfoliated 1D RP nanoribbons exhibit p-type behavior with a field-effect hole mobility of 236.7 $cm^2\ V^{-1}\ s^{-1}$ and an on/off current ratio of 1.6×10^3.[24] These results lay a solid foundation to further study their intrinsic electronic properties, highlighting that elemental RP may serve as an ideal channel material for high-performance FETs. On the other hand, elemental RP possesses a bandgap of 1.69 eV, close to iodine-based perovskites, which has the potential for achieving low-cost light absorption components (Figure 3b). Lately, 1D RP ACs were encapsulated within conductive and robust single-walled CNTs, by which their applications in ion batteries, supercapacitors, and photocatalysis were highlighted.[70]

In complementary technologies, extrinsic doping processes, such as ion implantation and thermal diffusion, are generally used to obtain p-type or n-type unipolar semiconductors. Besides, some exceptional cases of CNTs, layered 2D materials, and organic semiconductors could show ambipolar characteristics, as the concentrations of the electron and hole carriers are comparable. Notably, the exfoliated 1D $Ta_2Ni_3Se_8$ ACs demonstrated the ambipolar semiconducting behavior,[36] whereas the $Ta_2Pd_3Se_8$ and $Ta_2Pt_3Se_8$ ACs were found to exhibit n-type and p-type semiconducting characteristics, respectively.[49,71] It is unusual to observe different transport polarities in one isostructural material system, which can be conveniently integrated into complementary electronics (Figure 3c).[72] Also, the ambipolar semiconducting $Ta_2Ni_3Se_8$ ACs, featured with the differential transconductance under positive/negative gate bias, can enable the higher data processing capability in a single device, thus significantly simplifying the circuit design. Based on the same concept, nanoscale ambipolar or anti-ambipolar optoelectronic devices with multifunctionality have been demonstrated most recently.[73,74]

1D TiS_3 is broadly classified as an n-type semiconductor with a direct bandgap of ~1 eV.[75] The predicted mobility of TiS_3 is close to $\sim 10^4\ cm^2$ along the chain direction, more than an order of magnitude higher than that in the perpendicular direction, featuring an anisotropic carrier transport.[76] The narrow bandgap, high mobility, and large current carrying ability of 1D TiS_3 show its promise as a high-performance semiconducting channel. The observations on TiS_3 about charge density wave,[77] filamentary superconductivity, and field-induced metal−insulator transition (MIT)[78,79] have also received considerable attention. Significantly, the combination of high-mobility semiconductors and near-room-temperature MIT would generate a different type of transistor, known as a phase-change transistor (PCT). The fundamentally different mechanism for PCT switching can bypass the static and dynamic power consumption issues in conventional FETs.[80] Also, the PCT may transform the conventional computation architectures because the power, speed, and volatility considerations no longer exist.

Apart from charge carrier transport (i.e., electron and hole), fascinating phenomena are also observed when energy carriers (i.e., phonon) are confined in one dimension. Recently, experimental evidence of the transition from 3D to 1D phonon

https://doi.org/10.1021/acsnano.2c06359
ACS Nano 2022, 16, 13314−13322

transport was discovered in $NbSe_3$ ACs.[57] The unusual superdiffusive along-chain thermal transport was experimentally observed, including a divergent thermal conductivity (κ) $\sim L^{1/3}$ and a 25-fold κ enhancement to 109 $W\,m^{-1}\,k^{-1}$. The dominated 1D phonon transport is believed to result from the drastic elastic stiffening along the chain direction. In addition to the enhanced 1D thermal conductivity, it is found that the ballistic phonon transport can persist over 13 μm at room temperature and 17 μm at 55 K along the chain direction of 1D $Ta_2Pd_3Se_8$.[37] This value has outperformed the conventional materials, e.g., SiGe NWs of 8.3 μm[81] and single-wall CNT of ~10 μm,[82] corresponding to one of the longest experimentally observed ballistic phonon transport distances. Theoretical calculations propose that the ultralong ballistic phonon transport comes from the strongly focused longitudinal phonons propagating along the chain direction without being scattered.[37] The drastically enhanced thermal conductivity along 1D ACs would facilitate the phonon transport manipulation for "smart" thermoelectrics and efficient heat dissipation.

Spintronics fundamentally differ from traditional electronics, in which the electron spins and the associated magnetic moments in ferromagnets are utilized.[83] It is noted that many AC materials, such as TMC ACs in the stoichiometry of M_6X_6 (including Co_6S_6, Co_6Se_6, Co_6Te_6, Fe_6S_6, and Fe_6Se_6), are suggested to be 1D ferromagnets with a Curie temperature up to 700 K, being promising for room-temperature spintronic devices.[38] The enhanced efficiency of data storage and transfer in room-temperature ACs spintronics are of particular interest for quantum computing and neuromorphic computing. Most recently, the all-electrical generation, manipulation, and detection of spin polarization have been demonstrated in chiral single-crystalline 1D Te NWs, inspiring us to exploit chiral spintronic devices.[21] In addition to the electrostatic control, the strain effect can also be used to induce the reversible topological phase transition as observed in 1D superconducting $TaSe_3$ ACs, thus allowing for an on/off switching of spin current.[84] The interplay of topological phase transition with superconductivity in $TaSe_3$ ACs would promote the basic and technological research for engineering topological spintronics.

CONCLUSIONS AND PROSPECTS

Until now, many kinds of 1D AC material systems have been synthesized or predicted, including elemental chains (e.g., Te and Se), transition metal chalcogenides (e.g., $Ta_2Pt_3Se_8$ and Mo_6Te_6), transition metal halides (e.g., CoI_2 and $MoBr_3$), etc. The variable structural and compositional characteristics fundamentally determine the material properties of 1D ACs, by which it is possible to design and fabricate 1D ACs with desired band structures for target device applications. Importantly, these dangling-bond-free 1D ACs are expected to outperform the competitive channel materials for the ultimate-downscaled nanometer or even sub-nanometer electronics. Also, the ultrathin atomic-scale features of ACs make their electronic properties delicately regulated by different external stimuli, such as strain, light, thermal, magnetic, electric, or electrostatic effects. This versatility endows 1D ACs with application potential in not only electronic but also photonic, optoelectronic, thermoelectric, spintronic, and memory devices.

Currently, the investigation of inorganic 1D ACs is still in its infancy stage, especially the shortness of study on few-chain or single-chain materials; thus, many research opportunities exist. From a material viewpoint, rational design and fabrication of 1D ACs with desired material properties are needed to satisfy the specific applications. Particularly, the high-mobility transistors need a channel with a narrow bandgap <1 e V, while the optoelectronics require their light absorption component with sufficient thickness and appropriate bandgap. Also, solid-state chemistry methods are easily employed to alter the 1D AC properties, including compositions, doping, phases, and structures. The confinement and surface effect associated with the downscaling process can be considered to engineer the physical and electronic properties of 1D ACs deeply.

From a device viewpoint, exploring ultrathin 1D ACs for cutting-edge applications is meaningful. For instance, we may build the smallest memory device based on 1D ACs and, more importantly, identify the corresponding filamentary conductance quanta. Recently, the elemental Te-based resistive switching devices have attracted wide attention, while the operating mechanisms are generally explained from a macro perspective, e.g., Joule heat-induced phase transition.[85,86] If one can design 1D ACs as an individual filamentary resistive switch, the physical nature of filamentary conductance quanta may be uncovered to show more insights. The ACs filamentary switches would shrink the memory devices downscaling to the atomic scale, by which the data processing and memorizing will be more precise and fault-tolerant.

Based on the 1D vdW crystal structures with naturally terminated surfaces, AC systems have become a powerful platform for studying pure 1D physics, such as exotic quantum states, quantized conductance, ballistic phonon transport, Tomonaga–Luttinger liquid behavior, and charge-induced torsional instability. For example, with the help of angle-resolved photoemission spectroscopy, 1D metallic $TaSe_3$ ACs were observed to have various excitonic bound states, including intrachain and interchain excitons, and possibly trions, being useful as efficient transmitters of information.[87] In addition, the charge-induced torsional motion was recently discovered in $NbSe_3$ ACs[88] and MoTe ACs,[56] leading to distinctive optical and electron transport properties when torsional motion existed. Overall, the vdW bonding among ACs involves many-body physics dispersion interactions, whereas covalent bonding along a single chain involves strong electronic correlations and electron–phonon coupling.

Apart from the fabrication and utilization of 1D ACs, the capabilities to characterize their structures and properties are also urgently needed. While 2D materials with few-layer thickness located on a suitable substrate could be identified with optical microscopy, identifying 1D ACs using this method is likely not feasible. In some cases, the 1D ACs with different chain numbers are distinguishable by micro-Raman spectroscopy,[19] enabled by their highly anisotropic vdW-bonded 1D structure, which may partly address the challenge of identifying ACs after isolation. On the other hand, advanced computational techniques are also needed to fully understand the relationships among material compositions, geometrical structures, and electronic configurations in 1D ACs as well as to realize 1D AC predictions.

AUTHOR INFORMATION

Corresponding Author

Johnny C. Ho − *Department of Materials Science and Engineering and State Key Laboratory of Terahertz and*

https://doi.org/10.1021/acsnano.2c06359
ACS Nano 2022, 16, 13314−13322

Millimeter Waves, City University of Hong Kong, Kowloon 999077, Hong Kong SAR; Institute for Materials Chemistry and Engineering, Kyushu University, Fukuoka 816-8580, Japan; orcid.org/0000-0003-3000-8794;
Email: johnnyho@cityu.edu.hk

Authors

You Meng − *Department of Materials Science and Engineering and State Key Laboratory of Terahertz and Millimeter Waves, City University of Hong Kong, Kowloon 999077, Hong Kong SAR*

Wei Wang − *Department of Materials Science and Engineering, City University of Hong Kong, Kowloon 999077, Hong Kong SAR*

Complete contact information is available at: https://pubs.acs.org/10.1021/acsnano.2c06359

Notes

The authors declare no competing financial interest.

ACKNOWLEDGMENTS

This work is supported by a fellowship award from the Research Grants Council of the Hong Kong Special Administrative Region, China (CityU RFS2021-1S04).

REFERENCES

(1) Wu, F.; Tian, H.; Shen, Y.; Hou, Z.; Ren, J.; Gou, G.; Sun, Y.; Yang, Y.; Ren, T.-L. Vertical MoS_2 transistors with sub-1-nm gate lengths. *Nature* **2022**, *603* (7900), 259−264.
(2) Liu, Y.; Duan, X.; Shin, H.-J.; Park, S.; Huang, Y.; Duan, X. Promises and prospects of two-dimensional transistors. *Nature* **2021**, *591* (7848), 43−53.
(3) Lundstrom, M. Moore's Law Forever? *Science* **2003**, *299* (5604), 210−211.
(4) Moore, G. E. Cramming More Components Onto Integrated Circuits. *Proceedings of the IEEE* **1998**, *86* (1), 82−85.
(5) Chen, M.-L.; Sun, X.; Liu, H.; Wang, H.; Zhu, Q.; Wang, S.; Du, H.; Dong, B.; Zhang, J.; Sun, Y.; Qiu, S.; Alava, T.; Liu, S.; Sun, D.-M.; Han, Z. A FinFET with one atomic layer channel. *Nat. Commun.* **2020**, *11* (1), 1205.
(6) Desai, S. B.; Madhvapathy, S. R.; Sachid, A. B.; Llinas, J. P.; Wang, Q.; Ahn, G. H.; Pitner, G.; Kim, M. J.; Bokor, J.; Hu, C.; Wong, H.-S. P.; Javey, A. MoS_2 transistors with 1-nanometer gate lengths. *Science* **2016**, *354* (6308), 99−102.
(7) Lu, W.; Lee, Y.; Gertsch, J. C.; Murdzek, J. A.; Cavanagh, A. S.; Kong, L.; del Alamo, J. A.; George, S. M. In Situ Thermal Atomic Layer Etching for Sub-5 nm InGaAs Multigate MOSFETs. *Nano Lett.* **2019**, *19* (8), 5159−5166.
(8) Kramer, A.; Van de Put, M. L.; Hinkle, C. L.; Vandenberghe, W. G. Tellurium as a successor of silicon for extremely scaled nanowires: a first-principles study. *npj 2D Mater. Appl.* **2020**, *4* (1), 10.
(9) Franklin, A. D. Nanomaterials in transistors: From high-performance to thin-film applications. *Science* **2015**, *349* (6249), aab2750.
(10) Liu, Y.; Huang, Y.; Duan, X. Van der Waals integration before and beyond two-dimensional materials. *Nature* **2019**, *567* (7748), 323−333.
(11) Radisavljevic, B.; Radenovic, A.; Brivio, J.; Giacometti, V.; Kis, A. Single-layer MoS_2 transistors. *Nat. Nanotechnol.* **2011**, *6* (3), 147−150.
(12) Lee, H. W.; Yoon, Y.; Park, S.; Oh, J. H.; Hong, S.; Liyanage, L. S.; Wang, H.; Morishita, S.; Patil, N.; Park, Y. J.; Park, J. J.; Spakowitz, A.; Galli, G.; Gygi, F.; Wong, P. H. S.; Tok, J. B. H.; Kim, J. M.; Bao, Z. Selective dispersion of high purity semiconducting single-walled carbon nanotubes with regioregular poly(3-alkylthiophene)s. *Nat. Commun.* **2011**, *2* (1), 541.
(13) Jia, C.; Lin, Z.; Huang, Y.; Duan, X. Nanowire electronics: from nanoscale to macroscale. *Chem. Rev.* **2019**, *119* (15), 9074−9135.
(14) Li, D.; Lan, C.; Manikandan, A.; Yip, S.; Zhou, Z.; Liang, X.; Shu, L.; Chueh, Y.-L.; Han, N.; Ho, J. C. Ultra-fast photodetectors based on high-mobility indium gallium antimonide nanowires. *Nat. Commun.* **2019**, *10* (1), 1664.
(15) Meng, Y.; Li, F.; Lan, C.; Bu, X.; Kang, X.; Wei, R.; Yip, S.; Li, D.; Wang, F.; Takahashi, T.; Hosomi, T.; Nagashima, K.; Yanagida, T.; Ho, J. C. Artificial visual systems enabled by quasi−two-dimensional electron gases in oxide superlattice nanowires. *Sci. Adv.* **2020**, *6* (46), eabc6389.
(16) Cheon, G.; Duerloo, K.-A. N.; Sendek, A. D.; Porter, C.; Chen, Y.; Reed, E. J. Data mining for new two-and one-dimensional weakly bonded solids and lattice-commensurate heterostructures. *Nano Lett.* **2017**, *17* (3), 1915−1923.
(17) Zhu, Y.; Rehn, D. A.; Antoniuk, E. R.; Cheon, G.; Freitas, R.; Krishnapriyan, A.; Reed, E. J. Spectrum of Exfoliable 1D van der Waals Molecular Wires and Their Electronic Properties. *ACS Nano* **2021**, *15* (6), 9851−9859.
(18) Lu, F.; Cui, J.; Liu, P.; Lin, M.; Cheng, Y.; Liu, H.; Wang, W.; Cho, K.; Wang, W.-H. High-throughput identification of one-dimensional atomic wires and first principles calculations of their electronic states. *Chin. Phys. B* **2021**, *30* (5), No. 057304.
(19) Qin, J.-K.; Liao, P.-Y.; Si, M.; Gao, S.; Qiu, G.; Jian, J.; Wang, Q.; Zhang, S.-Q.; Huang, S.; Charnas, A. Raman response and transport properties of tellurium atomic chains encapsulated in nanotubes. *Nat. Electron.* **2020**, *3* (3), 141−147.
(20) Du, Y.; Qiu, G.; Wang, Y.; Si, M.; Xu, X.; Wu, W.; Ye, P. D. One-dimensional van der Waals material tellurium: Raman spectroscopy under strain and magneto-transport. *Nano Lett.* **2017**, *17* (6), 3965−3973.
(21) Calavalle, F.; Suárez-Rodríguez, M.; Martín-García, B.; Johansson, A.; Vaz, D. C.; Yang, H.; Maznichenko, I. V.; Ostanin, S.; Mateo-Alonso, A.; Chuvilin, A.; Mertig, I.; Gobbi, M.; Casanova, F.; Hueso, L. E. Gate-tuneable and chirality-dependent charge-to-spin conversion in tellurium nanowires. *Nat. Mater.* **2022**, *21* (5), 526−532.
(22) Terasaki, O.; Yamazaki, K.; Thomas, J.; Ohsuna, T.; Watanabe, D.; Sanders, J.; Barry, J. Isolating individual chains of selenium by incorporation into the channels of a zeolite. *Nature* **1987**, *330* (6143), 58−60.
(23) Fujimori, T.; Morelos-Gómez, A.; Zhu, Z.; Muramatsu, H.; Futamura, R.; Urita, K.; Terrones, M.; Hayashi, T.; Endo, M.; Young Hong, S. Conducting linear chains of sulphur inside carbon nanotubes. *Nat. Commun.* **2013**, *4* (1), 2162.
(24) Sun, Z.; Zhang, B.; Zhao, Y.; Khurram, M.; Yan, Q. Synthesis, Exfoliation, and Transport Properties of Quasi-1D van der Waals Fibrous Red Phosphorus. *Chem. Mater.* **2021**, *33* (15), 6240−6248.
(25) Shi, L.; Rohringer, P.; Suenaga, K.; Niimi, Y.; Kotakoski, J.; Meyer, J. C.; Peterlik, H.; Wanko, M.; Cahangirov, S.; Rubio, A. Confined linear carbon chains as a route to bulk carbyne. *Nat. Mater.* **2016**, *15* (6), 634−639.
(26) Yang, F.; Li, C.; Li, J.; Liu, P.; Yang, G. Carbyne Nanocrystal: One-Dimensional van der Waals Crystal. *ACS Nano* **2021**, *15* (10), 16769−16776.
(27) Liu, M.; Artyukhov, V. I.; Lee, H.; Xu, F.; Yakobson, B. I. Carbyne from first principles: chain of C atoms, a nanorod or a nanorope. *ACS Nano* **2013**, *7* (11), 10075−10082.
(28) Baughman, R. H. Dangerously seeking linear carbon. *Science* **2006**, *312* (5776), 1009−1110.
(29) Deng, J.; Huo, D.; Bai, Y.; Guo, Y.; Pan, Z.; Lu, S.; Cui, P.; Zhang, Z.; Zhang, C. Precise Tuning of Band Structures and Electron Correlations by van der Waals Stacking of One-dimensional W_6Te_6 Wires. *Nano Lett.* **2020**, *20* (12), 8866−8873.
(30) Lin, J.; Cretu, O.; Zhou, W.; Suenaga, K.; Prasai, D.; Bolotin, K. I.; Cuong, N. T.; Otani, M.; Okada, S.; Lupini, A. R. Flexible metallic nanowires with self-adaptive contacts to semiconducting transition-metal dichalcogenide monolayers. *Nat. Nanotechnol.* **2014**, *9* (6), 436−442.

(31) Thomson, J. W.; Cademartiri, L.; MacDonald, M.; Petrov, S.; Calestani, G.; Zhang, P.; Ozin, G. A. Ultrathin Bi_2S_3 Nanowires: Surface and Core Structure at the Cluster-Nanocrystal Transition. *J. Am. Chem. Soc.* **2010**, *132* (26), 9058−9068.
(32) Caruso, F.; Filip, M. R.; Giustino, F. Excitons in one-dimensional van der Waals materials: Sb_2S_3 nanoribbons. *Phys. Rev. B* **2015**, *92* (12), 125134.
(33) Lipatov, A.; Loes, M. J.; Lu, H.; Dai, J.; Patoka, P.; Vorobeva, N. S.; Muratov, D. S.; Ulrich, G.; Kästner, B.; Hoehl, A. Quasi-1D TiS_3 nanoribbons: mechanical exfoliation and thickness-dependent Raman spectroscopy. *ACS Nano* **2018**, *12* (12), 12713−12720.
(34) Stonemeyer, S.; Cain, J. D.; Oh, S.; Azizi, A.; Elasha, M.; Thiel, M.; Song, C.; Ercius, P.; Cohen, M. L.; Zettl, A. Stabilization of $NbTe_3$, VTe_3, and $TiTe_3$ via nanotube encapsulation. *J. Am. Chem. Soc.* **2021**, *143* (12), 4563−4568.
(35) Oh, S.; Chae, S.; Kim, B. J.; Siddiqa, A. J.; Choi, K. H.; Jang, W.-S.; Lee, K. H.; Kim, H. Y.; Lee, D. K.; Kim, Y.-M.; Yu, H. K.; Choi, J.-Y. Inorganic Molecular Chain Nb_2Se_9: Synthesis of Bulk Crystal and One-Atom-Thick Level Exfoliation. *Phys. Status Solidi RRL* **2018**, *12* (12), 1800451.
(36) Choi, K. H.; Jeong, B. J.; Jeon, J.; Chung, Y. K.; Sung, D.; Yoon, S. O.; Chae, S.; Kim, B. J.; Oh, S.; Lee, S. H. $Ta_2Ni_3Se_8$:1D van der Waals Material with Ambipolar Behavior. *Small* **2021**, *17* (37), 2102602.
(37) Zhang, Q.; Liu, C.; Liu, X.; Liu, J.; Cui, Z.; Zhang, Y.; Yang, L.; Zhao, Y.; Xu, T. T.; Chen, Y.; Wei, J.; Mao, Z.; Li, D. Thermal Transport in Quasi-1D van der Waals Crystal $Ta_2Pd_3Se_8$ Nanowires: Size and Length Dependence. *ACS Nano* **2018**, *12* (3), 2634−2642.
(38) Shang, C.; Fu, L.; Zhou, S.; Zhao, J. Atomic Wires of transition metal chalcogenides: A family of 1D materials for flexible electronics and spintronics. *JACS Au* **2021**, *1* (2), 147−155.
(39) Philp, E.; Sloan, J.; Kirkland, A. I.; Meyer, R. R.; Friedrichs, S.; Hutchison, J. L.; Green, M. L. H. An encapsulated helical one-dimensional cobalt iodide nanostructure. *Nat. Mater.* **2003**, *2* (12), 788−791.
(40) Hermann, A.; Vest, B.; Schwerdtfeger, P. Density functional study of $CrCl_2$: Structural, electronic, and magnetic properties. *Phys. Rev. B* **2006**, *74* (22), 224402.
(41) Merlino, S.; Labella, L.; Marchetti, F.; Toscani, S. Order−Disorder Transformation in $RuBr_3$ and $MoBr_3$: A Two-Dimensional Ising Model. *Chem. Mater.* **2004**, *16* (20), 3895−3903.
(42) Kitaura, R.; Ogawa, D.; Kobayashi, k.; Saito, T.; Ohshima, S.; Nakamura, T.; Yoshikawa, H.; Awaga, K.; Shinohara, H. High yield synthesis and characterization of the structural and magnetic properties of crystalline $ErCl_3$ nanowires in single-walled carbon nanotube templates. *Nano Res.* **2008**, *1* (2), 152−157.
(43) Fu, L.; Shang, C.; Zhou, S.; Guo, Y.; Zhao, J. Transition metal halide nanowires: A family of one-dimensional multifunctional building blocks. *Appl. Phys. Lett.* **2022**, *120* (2), No. 023103.
(44) Meng, Y.; Lai, Z.; Li, F.; Wang, W.; Yip, S.; Quan, Q.; Bu, X.; Wang, F.; Bao, Y.; Hosomi, T. Perovskite Core−Shell Nanowire Transistors: Interfacial Transfer Doping and Surface Passivation. *ACS Nano* **2020**, *14* (10), 12749−12760.
(45) Meng, Y.; Lan, C.; Li, F.; Yip, S.; Wei, R.; Kang, X.; Bu, X.; Dong, R.; Zhang, H.; Ho, J. C. Direct Vapor−Liquid−Solid Synthesis of All-Inorganic Perovskite Nanowires for High-Performance Electronics and Optoelectronics. *ACS Nano* **2019**, *13* (5), 6060−6070.
(46) Wang, W.; Dai, S.; Li, X.; Yang, J.; Srolovitz, D. J.; Zheng, Q. Measurement of the cleavage energy of graphite. *Nat. Commun.* **2015**, *6* (1), 7853.
(47) Jin, Y.; Li, X.; Yang, J. Single layer of MX_3 (M= Ti, Zr; X= S, Se, Te): a new platform for nano-electronics and optics. *Phys. Chem. Chem. Phys.* **2015**, *17* (28), 18665−18669.
(48) Churchill, H. O.; Salamo, G. J.; Yu, S.-Q.; Hironaka, T.; Hu, X.; Stacy, J.; Shih, I. Toward single atom chains with exfoliated tellurium. *Nanoscale Res. Lett.* **2017**, *12* (1), 488.
(49) Jeong, B. J.; Choi, K. H.; Jeon, J.; Yoon, S. O.; Chung, Y. K.; Sung, D.; Chae, S.; Oh, S.; Kim, B. J.; Lee, S. H. One-dimensional van der Waals stacked p-type crystal $Ta_2Pt_3Se_8$ for nanoscale electronics. *Nanoscale* **2021**, *13* (42), 17945−17952.
(50) Liu, X.; Liu, S.; Antipina, L. Y.; Zhu, Y.; Ning, J.; Liu, J.; Yue, C.; Joshy, A.; Zhu, Y.; Sun, J.; Sanchez, A. M.; Sorokin, P. B.; Mao, Z.; Xiong, Q.; Wei, J. High yield production of ultrathin fibroid semiconducting nanowire of $Ta_2Pd_3Se_8$. *Nano Res.* **2020**, *13* (6), 1627−1635.
(51) Lim, H. E.; Nakanishi, Y.; Liu, Z.; Pu, J.; Maruyama, M.; Endo, T.; Ando, C.; Shimizu, H.; Yanagi, K.; Okada, S. Wafer-Scale Growth of One-Dimensional Transition-Metal Telluride Nanowires. *Nano Lett.* **2021**, *21* (1), 243−249.
(52) Yoo, Y.; Jeong, J. S.; Ma, R.; Koester, S. J.; Johns, J. E. Ultrathin One-Dimensional Molybdenum Telluride Quantum Wires Synthesized by Chemical Vapor Deposition. *Chem. Mater.* **2020**, *32* (22), 9650−9655.
(53) Lin, J.; Zhang, Y.; Zhou, W.; Pantelides, S. T. Structural flexibility and alloying in ultrathin transition-metal chalcogenide nanowires. *ACS Nano* **2016**, *10* (2), 2782−2790.
(54) Li, F.; Meng, Y.; Dong, R.; Yip, S.; Lan, C.; Kang, X.; Wang, F.; Chan, K. S.; Ho, J. C. High-Performance Transparent Ultraviolet Photodetectors Based on InGaZnO Superlattice Nanowire Arrays. *ACS Nano* **2019**, *13* (10), 12042−12051.
(55) Li, X.; Meng, Y.; Fan, R.; Fan, S.; Dang, C.; Feng, X.; Ho, J. C.; Lu, Y. High elasticity of $CsPbBr_3$ perovskite nanowires for flexible electronics. *Nano Res.* **2021**, *14*, 4033−4037.
(56) Nagata, M.; Shukla, S.; Nakanishi, Y.; Liu, Z.; Lin, Y.-C.; Shiga, T.; Nakamura, Y.; Koyama, T.; Kishida, H.; Inoue, T.; Kanda, N.; Ohno, S.; Sakagawa, Y.; Suenaga, K.; Shinohara, H. Isolation of Single-Wired Transition-Metal Monochalcogenides by Carbon Nanotubes. *Nano Lett.* **2019**, *19* (8), 4845−4851.
(57) Yang, L.; Tao, Y.; Zhu, Y.; Akter, M.; Wang, K.; Pan, Z.; Zhao, Y.; Zhang, Q.; Xu, Y.-Q.; Chen, R. Observation of superdiffusive phonon transport in aligned atomic chains. *Nat. Nanotechnol.* **2021**, *16* (7), 764−768.
(58) Slade, C. A.; Sanchez, A. M.; Sloan, J. Unprecedented new crystalline forms of SnSe in narrow to medium diameter carbon nanotubes. *Nano Lett.* **2019**, *19* (5), 2979−2984.
(59) Kashtiban, R. J.; Burdanova, M. G.; Vasylenko, A.; Wynn, J.; Medeiros, P. V.; Ramasse, Q.; Morris, A. J.; Quigley, D.; Lloyd-Hughes, J.; Sloan, J. Linear and Helical Cesium Iodide Atomic Chains in Ultranarrow Single-Walled Carbon Nanotubes: Impact on Optical Properties. *ACS Nano* **2021**, *15* (8), 13389−13398.
(60) Cain, J. D.; Oh, S.; Azizi, A.; Stonemeyer, S.; Dogan, M.; Thiel, M.; Ercius, P.; Cohen, M. L.; Zettl, A. Ultranarrow TaS_2 Nanoribbons. *Nano Lett.* **2021**, *21* (7), 3211−3217.
(61) Stonemeyer, S.; Dogan, M.; Cain, J. D.; Azizi, A.; Popple, D. C.; Culp, A.; Song, C.; Ercius, P.; Cohen, M. L.; Zettl, A. Targeting One- and Two-Dimensional Ta−Te Structures via Nanotube Encapsulation. *Nano Lett.* **2022**, *22* (6), 2285−2292.
(62) Dasika, P.; Samantaray, D.; Murali, K.; Abraham, N.; Watanbe, K.; Taniguchi, T.; Ravishankar, N.; Majumdar, K. Contact-Barrier Free, High Mobility, Dual-Gated Junctionless Transistor Using Tellurium Nanowire. *Adv. Funct. Mater.* **2021**, *31* (13), 2006278.
(63) Qiao, J.; Pan, Y.; Yang, F.; Wang, C.; Chai, Y.; Ji, W. Few-layer Tellurium: one-dimensional-like layered elementary semiconductor with striking physical properties. *Sci. Bull.* **2018**, *63* (3), 159−168.
(64) Tan, C.; Amani, M.; Zhao, C.; Hettick, M.; Song, X.; Lien, D. H.; Li, H.; Yeh, M.; Shrestha, V. R.; Crozier, K. B.; Scott, M. C.; Javey, A. Evaporated Se_xTe_{1-x} Thin Films with Tunable Bandgaps for Short Wave Infrared Photodetectors. *Adv. Mater.* **2020**, *32*, 2001329.
(65) Jena, D.; Konar, A. Enhancement of carrier mobility in semiconductor nanostructures by dielectric engineering. *Phys. Rev. Lett.* **2007**, *98* (13), 136805.
(66) Liu, Y.; Liu, Q.; Jian, C.; Cui, D.; Chen, M.; Li, Z.; Li, T.; Nilges, T.; He, K.; Jia, Z.; Zhou, C. Red-phosphorus-impregnated carbon nanofibers for sodium-ion batteries and liquefaction of red phosphorus. *Nat. Commun.* **2020**, *11* (1), 2520.

https://doi.org/10.1021/acsnano.2c06359
ACS Nano 2022, 16, 13314−13322

(67) Qian, J.; Wu, X.; Cao, Y.; Ai, X.; Yang, H. High Capacity and Rate Capability of Amorphous Phosphorus for Sodium Ion Batteries. *Angew. Chem., Int. Ed.* **2013**, *52* (17), 4633−4636.
(68) Amaral, P. E. M.; Nieman, G. P.; Schwenk, G. R.; Jing, H.; Zhang, R.; Cerkez, E. B.; Strongin, D.; Ji, H.-F. High Electron Mobility of Amorphous Red Phosphorus Thin Films. *Angew. Chem., Int. Ed.* **2019**, *58* (20), 6766−6771.
(69) Ban, H. W.; Oh, J. G.; Jo, S.; Jeong, H.; Gu, D. H.; Baek, S.; Lee, S. Y.; Park, Y. I.; Jang, J.; Son, J. S. Polyphosphide Precursor for Low-Temperature Solution-Processed Fibrous Phosphorus Thin Films. *Chem. Mater.* **2019**, *31* (15), 5909−5918.
(70) Rybkovskiy, D.; Koroteev, V.; Impellizzeri, A.; Vorfolomeeva, A.; Gerasimov, E. Y.; Okotrub, A.; Chuvilin, A.; Bulusheva, L.; Ewels, C. "Missing" One-Dimensional Red-Phosphorus Chains Encapsulated within Single-Walled Carbon Nanotubes. *ACS Nano* **2022**, *16* (4), 6002−6012.
(71) Jeong, B. J.; Choi, K. H.; Jeon, J.; Yoon, S. O.; Chung, Y. K.; Sung, D.; Chae, S.; Kim, B. J.; Oh, S.; Lee, S. H. Ternary transition metal chalcogenide $Nb_2Pd_3Se_8$: a new candidate of 1D van der Waals materials for field-effect transistors. *Adv. Funct. Mater.* **2022**, *32* (4), 2108104.
(72) Liu, X.; Liu, J.; Antipina, L. Y.; Hu, J.; Yue, C.; Sanchez, A. M.; Sorokin, P. B.; Mao, Z.; Wei, J. Direct Fabrication of Functional Ultrathin Single-Crystal Nanowires from Quasi-One-Dimensional van der Waals Crystals. *Nano Lett.* **2016**, *16* (10), 6188−6195.
(73) Wang, W.; Wang, W.; Meng, Y.; Quan, Q.; Lai, Z.; Li, D.; Xie, P.; Yip, S.; Kang, X.; Bu, X.; Chen, D.; Liu, C.; Ho, J. C. Mixed-Dimensional Anti-ambipolar Phototransistors Based on 1D GaAsSb/2D MoS_2 Heterojunctions. *ACS Nano* **2022**, *16* (7), 11036−11048.
(74) Wang, W.; Meng, Y.; Wang, W.; Zhang, Z.; Xie, P.; Lai, Z.; Bu, X.; Li, Y.; Liu, C.; Yang, Z.; Yip, S.; Ho, J. C. Highly Efficient Full van der Waals 1D p-Te/2D n-Bi_2O_2Se Heterodiodes with Nanoscale Ultra-Photosensitive Channels. *Adv. Funct. Mater.* **2022**, *32*, 2203003.
(75) Island, J. O.; Barawi, M.; Biele, R.; Almazán, A.; Clamagirand, J. M.; Ares, J. R.; Sánchez, C.; van der Zant, H. S. J.; Álvarez, J. V.; D'Agosta, R.; Ferrer, I. J.; Castellanos-Gomez, A. TiS_3 Transistors with Tailored Morphology and Electrical Properties. *Adv. Mater.* **2015**, *27* (16), 2595−2601.
(76) Dai, J.; Zeng, X. C. Titanium Trisulfide Monolayer: Theoretical Prediction of a New Direct-Gap Semiconductor with High and Anisotropic Carrier Mobility. *Angew. Chem., Int. Ed.* **2015**, *54* (26), 7572−7576.
(77) Randle, M. D.; Lipatov, A.; Mansaray, I.; Han, J. E.; Sinitskii, A.; Bird, J. P. Collective states and charge density waves in the group IV transition metal trichalcogenides. *Appl. Phys. Lett.* **2021**, *118* (21), 210502.
(78) Randle, M. D.; Lipatov, A.; Datta, A.; Kumar, A.; Mansaray, I.; Sinitskii, A.; Singisetti, U.; Han, J. E.; Bird, J. P. High-electric-field behavior of the metal-insulator transition in TiS_3 nanowire transistors. *Appl. Phys. Lett.* **2022**, *120* (7), No. 073102.
(79) Randle, M.; Lipatov, A.; Kumar, A.; Kwan, C.-P.; Nathawat, J.; Barut, B.; Yin, S.; He, K.; Arabchigavkani, N.; Dixit, R.; Komesu, T.; Avila, J.; Asensio, M. C.; Dowben, P. A.; Sinitskii, A.; Singisetti, U.; Bird, J. P. Gate-Controlled Metal−Insulator Transition in TiS_3 Nanowire Field-Effect Transistors. *ACS Nano* **2019**, *13* (1), 803−811.
(80) Hou, W.; Azizimanesh, A.; Sewaket, A.; Peña, T.; Watson, C.; Liu, M.; Askari, H.; Wu, S. M. Strain-based room-temperature non-volatile $MoTe_2$ ferroelectric phase change transistor. *Nat. Nanotechnol.* **2019**, *14* (7), 668−673.
(81) Hsiao, T.-K.; Chang, H.-K.; Liou, S.-C.; Chu, M.-W.; Lee, S.-C.; Chang, C.-W. Observation of room-temperature ballistic thermal conduction persisting over 8.3 μm in SiGe nanowires. *Nat. Nanotechnol.* **2013**, *8* (7), 534−538.
(82) Liu, J.; Li, T.; Hu, Y.; Zhang, X. Benchmark study of the length dependent thermal conductivity of individual suspended, pristine SWCNTs. *Nanoscale* **2017**, *9* (4), 1496−1501.
(83) Li, X.; Yang, J. First-principles design of spintronics materials. *Natl. Sci. Rev.* **2016**, *3* (3), 365−381.
(84) Lin, C.; Ochi, M.; Noguchi, R.; Kuroda, K.; Sakoda, M.; Nomura, A.; Tsubota, M.; Zhang, P.; Bareille, C.; Kurokawa, K.; Arai, Y.; Kawaguchi, K.; Tanaka, H.; Yaji, K.; Harasawa, A.; Hashimoto, M.; Lu, D.; Shin, S.; Arita, R.; Tanda, S.; Kondo, T. Visualization of the strain-induced topological phase transition in a quasi-one-dimensional superconductor $TaSe_3$. *Nat. Mater.* **2021**, *20* (8), 1093−1099.
(85) Shen, J.; Jia, S.; Shi, N.; Ge, Q.; Gotoh, T.; Lv, S.; Liu, Q.; Dronskowski, R.; Elliott Stephen, R.; Song, Z.; Zhu, M. Elemental electrical switch enabling phase segregation−free operation. *Science* **2021**, *374* (6573), 1390−1394.
(86) Yang, Y.; Xu, M.; Jia, S.; Wang, B.; Xu, L.; Wang, X.; Liu, H.; Liu, Y.; Guo, Y.; Wang, L.; Duan, S.; Liu, K.; Zhu, M.; Pei, J.; Duan, W.; Liu, D.; Li, H. A new opportunity for the emerging tellurium semiconductor: making resistive switching devices. *Nat. Commun.* **2021**, *12* (1), 6081.
(87) Ma, J.; Nie, S.; Gui, X.; Naamneh, M.; Jandke, J.; Xi, C.; Zhang, J.; Shang, T.; Xiong, Y.; Kapon, I.; Kumar, N.; Soh, Y.; Gosálbez-Martínez, D.; Yazyev, O. V.; Fan, W.; Hübener, H.; Giovannini, U. D.; Plumb, N. C.; Radovic, M.; Sentef, M. A.; Xie, W.; Wang, Z.; Mudry, C.; Müller, M.; Shi, M. Multiple mobile excitons manifested as sidebands in quasi-one-dimensional metallic $TaSe_3$. *Nat. Mater.* **2022**, *21* (4), 423−429.
(88) Pham, T.; Oh, S.; Stetz, P.; Onishi, S.; Kisielowski, C.; Cohen, M. L.; Zettl, A. Torsional instability in the single-chain limit of a transition metal trichalcogenide. *Science* **2018**, *361* (6399), 263−266.

https://doi.org/10.1021/acsnano.2c06359
ACS Nano 2022, 16, 13314−13322